

Letter

Ton G. van Leeuwen*, Imran B. Akca, Nikolaos Angelou, Nicolas Weiss, Marcel Hoekman, Arne Leinse and Rene G. Heideman

On-chip Mach-Zehnder interferometer for OCT systems

<https://doi.org/10.1515/aot-2017-0061>

Received September 14, 2017; accepted November 27, 2017; previously published online January 6, 2018

Abstract: By using integrated optics, it is possible to reduce the size and cost of a bulky optical coherence tomography (OCT) system. One of the OCT components that can be implemented on-chip is the interferometer. In this work, we present the design and characterization of a Mach-Zehnder interferometer consisting of the wavelength-independent splitters and an on-chip reference arm. The Si_3N_4 was chosen as the material platform as it can provide low losses while keeping the device size small. The device was characterized by using a home-built swept source OCT system. A sensitivity value of 83 dB, an axial resolution of 15.2 μm (in air) and a depth range of 2.5 mm (in air) were all obtained.

Keywords: Mach-Zehnder interferometer; on-chip; optical coherence tomography; silicon nitride.

1 Introduction

Optical coherence tomography (OCT) is a minimally invasive optical imaging technique that provides high-resolution,

*Corresponding author: Ton G. van Leeuwen, Biomedical Engineering and Physics, Academic Medical Center, University of Amsterdam, Amsterdam, The Netherlands, e-mail: T.G.vanLeeuwen@amc.uva.nl

Imran B. Akca: Biomedical Engineering and Physics, Academic Medical Center, University of Amsterdam, P.O. Box 22700, Amsterdam 1100 DE, The Netherlands; and Institute for Lasers, Life and Biophotonics Amsterdam, Department of Physics and Astronomy, VU University Amsterdam, De Boelelaan, Amsterdam, The Netherlands

Nikolaos Angelou and Nicolas Weiss: Biomedical Engineering and Physics, Academic Medical Center, University of Amsterdam, Amsterdam, The Netherlands

Marcel Hoekman, Arne Leinse and Rene G. Heideman: Lionix International BV, Enschede AL, The Netherlands

www.degruyter.com/aot

© 2018 THOSS Media and De Gruyter

cross-sectional images of tissues and turbid media [1]. OCT can provide real-time images of tissues *in situ* and can advantageously be used where conventional excisional biopsies are hazardous or impossible. Although the current OCT systems are bulky and expensive, integrated optics offers unique solutions for OCT systems.

One of the OCT components that can be implemented on-chip is the interferometer. Various interferometer configurations using different material systems have been investigated by several research groups. Culemann et al. [2] reported the parallel integration of eight Michelson interferometers implemented in glass. Yurtsever et al. [3] demonstrated a Michelson interferometer implemented in silicon on insulator and a silicon nitride (Si_3N_4)-based Mach-Zehnder interferometer with a 190-mm-long on-chip reference arm [4]. Nguyen et al. [5] fabricated a Michelson interferometer in a Si_3N_4 platform to be used in a swept-source OCT system for *in vitro* tissue phantom imaging. In another study, Akca et al. [6] demonstrated a partially-integrated spectral-domain OCT system in silicon oxynitride (SiON).

In the present work, we present the design and characterization of a Mach-Zehnder interferometer consisting of the wavelength-independent splitters and an on-chip reference arm. Furthermore, two adjacent waveguides were used on the sample arm side: one for delivering the light and the other for collecting back scattered light from sample, which can circumvent the use of Y splitters and their additional (6 dB) losses. The device was characterized by using a home-built SS-OCT system with a center wavelength of 1550 nm. Results indicate that a sensitivity value of 83 dB, an axial resolution of 15.2 μm (in air) and a depth range of 2.5 mm (in air) were all obtained.

2 Chip design

2.1 Waveguide design

Here, Si_3N_4 was chosen as the material technology for this specific design as it can provide low-loss, compact and

reproducible waveguides. Moreover, it has a wide transparency range. A special waveguide type called TriPleX™ was used, which was developed by LioniX International BV (Enschede, The Netherlands) [7]. The waveguide geometry is a single-strip Si_3N_4 of 50 nm height and $3.4 \mu\text{m}$ width. The top and bottom SiO_2 cladding layers are $8 \mu\text{m}$ thick. Waveguides operate in single mode at a wavelength of 1550 nm and have a minimum bending loss for TE polarization. The refractive index contrast between Si_3N_4 ($n=1.98$) and SiO_2 ($n=1.45$) enables the realization of smaller device sizes.

2.2 Interferometer layout

Figure 1 presents the schematic of the integrated-optics-based SS-OCT system, in which the micro-chip is outlined by the red dashed-rectangle. The micro-chip consists of an on-chip Mach-Zehnder interferometer. The top and bottom waveguides are reference waveguides that are designed for estimating the fiber coupling losses. The characterization of the interferometer was performed by coupling the input light into the second waveguide from the top which is then equally split into two in the first splitter (s1) towards the reference and sample arms. The back-scattered light from the sample mirror was collected with the same waveguide (wg1) and then combined with the reference light at the splitter (s4), which was then divided equally for balanced detection. For the biological specimen measurements, the waveguide adjacent to the delivery waveguide (wg2) can be used for back-scattered light collection, which can then be combined with the reference light at the splitter (s5) for balanced detection. Using this path reduces the number of splitters that the back-scattered light passes, thereby increasing the system sensitivity by decreasing the splitter-induced losses. The physical length of the on-chip

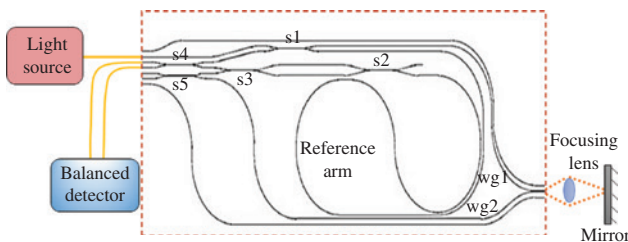


Figure 1: The schematic of the integrated-optics-based SS-OCT system in which the on-chip Mach-Zehnder interferometer micro-chip is outlined by the red dashed-rectangle. s1, s2, s3, s4, s5 correspond to the splitters, and wg1, wg2 correspond to the waveguides.

reference arm was designed to be 9.2 cm and the overall chip size was $1.7 \text{ cm} \times 0.5 \text{ cm}$.

The light source was a swept laser (Insight Photonic Solutions, Inc, Lafayette, CO, USA) with a 1550-nm center wavelength, 115-nm full width half maximum (FWHM) bandwidth, 7-mW average power and 50-kHz repetition rate. All splitters in the circuit were wavelength independent splitters with a 50/50 splitting ratio over the FWHM of the laser source. The light from the chip end was focused on the mirror by using an aspheric focusing lens. In order to cancel the RIN noise, a balanced detector was used (PDB40C, Thorlabs, Newton, USA). The interferometric data were sampled by a digitization card (ATS9350, Alazar Technologies Inc, Pointe-Claire, QC, Canada) at 500 MS/s. The ADC was used to digitize the measured intensities with an internal k-clock onto the 8000 samples.

3 Device characterization

3.1 Axial resolution

To characterize the system's axial resolution and sensitivity, a mirror was positioned at 0.1 mm. The measured raw interference and background spectra for a fixed mirror position are shown in Figure 2A and B, respectively, along with the corresponding calculated OCT signal (Figure 2C). We observed some high-frequency interference patterns both on the interference and background spectrum, which can be attributed to the back reflections originating from the chip end facet that was not angle polished (as shown in the insets). The data processing consisted of background subtraction, k-space resampling, Hilbert transform, Fourier transform and dispersion compensation. The dispersion mismatch between the two arms of the system was compensated in the software by applying the third-order polynomial approach. The measured axial resolution of the system was $15.2 \mu\text{m}$, larger than the theoretical axial resolution value of $9.2 \mu\text{m}$. This can be due to insufficient dispersion compensation as well as the reduced bandwidth of the wavelength-independent splitters.

3.2 Sensitivity

The ratio between the OCT point spread function at a 0.1-mm distance from the zero-delay point and the standard deviation of the noise floor gives the sensitivity of the system. The measured sensitivity of this system with

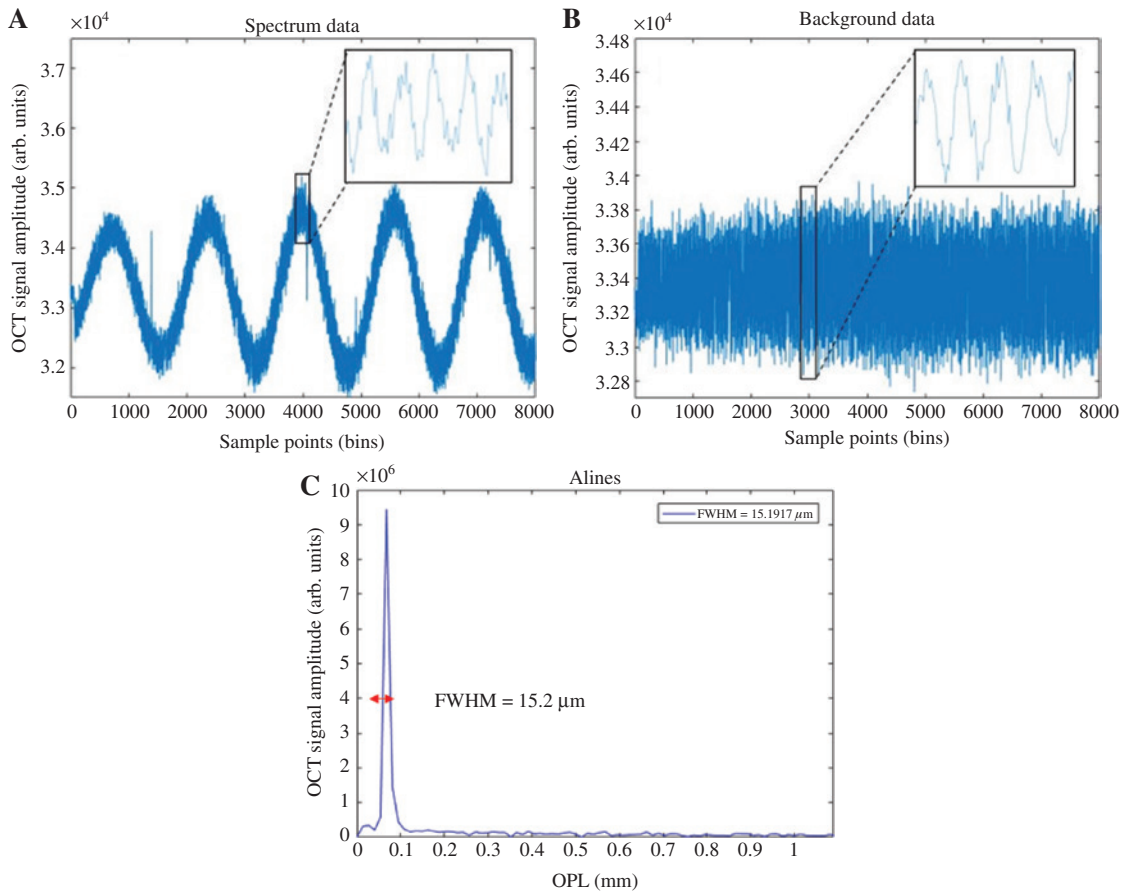


Figure 2: The characterization of the on-chip Mach-Zehnder interferometer implemented in the SS-OCT system. (A) Measured raw interference spectrum, and (B) background spectrum. The insets show the small interference coming from the chip facet. (C) Magnitude of the OCT signal. The FWHM of the peak is 15.2 μm .

0.25 mW on the sample was 83 dB, whereas the shot noise limited, lossless system would had a sensitivity of 110 dB. The total signal power measured on the balanced detector side was 90 μW , of which 50 μW originated from the reference arm when the sample arm was blocked. Consequently, 40 μW originated from the back-reflected light from the mirror into the sample arm. All power values were measured at 1569 nm. The power values at the balanced detector arms were 27 μW and 23 μW . The setup had total of 13 dB loss in the sample arm, due the losses at the input/output coupling of the chip, splitters and the focusing lens. Nevertheless, the system performance is comparable with that of a commercial SS-OCT system.

Figure 3 shows the measured OCT signals for nine different positions of the sample arm mirror, each separated by 250 μm . The observed decay in the amplitude with increasing optical path length can be attributed to the confocal gate of the focusing lens. Consequently, the maximum imaging range with this lens configuration was approximately 2.5 mm.

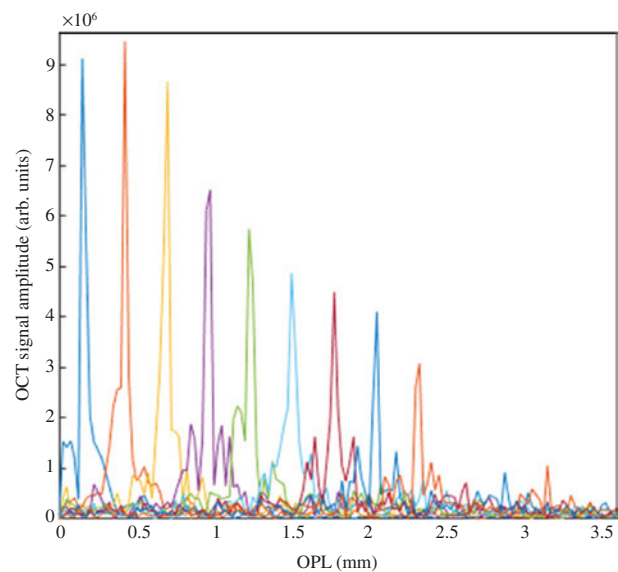


Figure 3: Measured A lines for nine different mirror positions. The maximum imaging range is around 2.5 mm.

4 Discussion

We have demonstrated an on-chip Mach-Zehnder interferometer with a high potential for OCT imaging based on photonic integrated components. However, some aspects still need to be improved for further integration with other OCT components. First, the 83-dB sensitivity of the system is still too low. In order to increase the system sensitivity, the input fiber coupling losses due to the spot size mismatches must be reduced significantly. These reductions can be obtained by using a lensed fiber or a spot size converter [8]. Second, the noise in the OCT signals should be reduced. An important improvement will be expected by angle polishing the end facets in order to reduce the back reflections. The temperature fluctuations may also contribute to the noise. However, the thermo-optic coefficient of the Si₃N₄ material is very small ($\sim 3 \times 10^{-5}$ RIU/°C). Consequently, thermal fluctuations will only result in small changes in the effective refractive indexes of the waveguides. The splitters are also highly fabrication-tolerant, therefore, their operation will not be affected by this small change in the index of the refraction as well. Still, if further reduction of the thermal dependency is required, the thermal control by means of a TEC can be incorporated. Third, although the 83-dB sensitivity of the system is capable of acquiring high-quality *in vivo* OCT images, an x-y scanner unit could not be accommodated between the sample and the focusing lens due to the limited spacing between them. This issue can be solved by increasing the on-chip reference arm length. However, this latter adjustment will have an effect on the dispersion mismatch between the sample and the reference arm. Although the dispersion compensation was not a big challenge in this design, for larger arm length mismatches, an advanced software compensation will be needed. Next to these software solutions, hardware solutions are also possible, e.g. by controlling the waveguide dispersion by changing the geometry of the waveguide, as proposed in [4].

Our design still features a chip in a lab rather than a lab-on-a-chip, but the integration of further OCT components on a common chip will be feasible. The integrated microlenses can replace bulky focusing lenses. The hybrid integration of active materials, e.g. wafer bonding techniques, can be exploited to integrate the light source and the detector array. The inclusion of the scanner unit, e.g. by MEMS technology and on-chip opto-electronic circuitry

for processing may complete the system integration. Considering the ability of lithography to mass-produce the optimized optical systems, the on-chip integration will pave the road towards a much wider distribution of OCT systems.

5 Conclusion

We have demonstrated an on-chip Mach-Zehnder interferometer to be used in OCT imaging. Although a sensitivity value of 83 dB was obtained, which was not too far from commercial system sensitivity values, better sensitivity values can be achieved by optimizing the design and fabrication methods. Considering the ability of lithography to mass-produce the optimized optical systems, the on-chip integration will pave the road towards a much wider distribution of OCT systems.

Acknowledgments: This work was supported by the IOP Photonic Devices program (managed by Agentschap NL), the Innovational Research Incentives Scheme Veni (SH302031, managed by NWO-TTW) and by the Marie Skłodowska Curie Individual Fellowships (FOIPO 704364). We thank Frank Coumans for the design of the interferometer and Naser Hosseini for the simulations and the design of the mask set.

References

- [1] D. Huang, E. A. Swanson, C. P. Lin, J. S. Schuman, W. G. Stinson, et al., *Science* 254, 1178 (1991).
- [2] D. Culemann, A. Knuettel and E. Voges, *IEEE J. Sel. Top. Quantum Electron.* 6(5), 730–734 (2000).
- [3] G. Yurtsever, K. Komorowska and R. Baets, *Proc. SPIE* 8091, 80910 (2011).
- [4] G. Yurtsever, B. Považay, A. Alex, B. Zabihian, W. Drexler, et al., *Biomed. Opt. Express* 5, 1050 (2014).
- [5] V. D. Nguyen, N. Weiss, W. Beeker, M. Hoekman, A. Leinse, et al., *Opt. Lett.* 37(23), 4820–4822 (2012).
- [6] B. I. Akca, B. Považay, A. Alex, K. Wörhoff, R. M. de Ridder, et al., *Opt. Express* 21(14), 16648–16656 (2013).
- [7] F. Morichetti, A. Melloni, M. Martinelli, R. G. Heideman, A. Leinse, et al., *J. Lightwave Technol.* 25(9), 2579–2589 (2007).
- [8] I. Moerman, P. P. Van Daele and P. M. Demeester, *IEEE J. Sel. Top. Quantum Electron.* 3(6), 13081320 (1997).